8th Australasian Congress on Applied Mechanics, ACAM 8
23-26 November 2014, Melbourne, Australia

Effect of weave structure on flax fibres reinforced polypropylene composites in stamp forming

Wentian Wang[1*], Adrian Lowe[2], Shankar Kalyanasundaram[3]

[a,b,c]*Research School of Engineering, Australian National University, North Road, Canberra 0200, Australia*

[*]*Corresponding author. Email: wentian.wang@anu.edu.au*

Abstract: This study investigates the effect of weave structure on flax fibre reinforced polypropylene composites in stamp forming, and develops FEA models to simulate the forming behaviour of composites. In this study, composites were fixed completely at the flange region and then formed into a hemispherical dome through a custom built stamping machine. Samples with different aspect ratio were investigated to obtain different major forming paths exhibited in composites. The ARAMIS™ system uses two high-resolution CCD (Charge-coupled device) cameras to monitor the surface motion of specimens and calculates displacement and strain deformation at every stage using photogrammetric methodologies. Experimental observations were used to validate the FEA simulations developed in this study. Numerical simulations can accurately simulate strain evolutions of composites with varying geometries, and successfully predict the effect of weave structure on natural fibre composites in stamp forming.

Keywords: Finite element model, Natural fibre composite, Stamp forming, Strain evolution.

1 Introduction

Globally, there is an urgent need to reduce the weight of vehicles to improve their fuel efficiencies, and to lower their environmental impacts. In addition to this, a large portion of vehicle panels will be required to be manufactured through recyclable and reusable material in a foreseeable future. The directive issued by the end of life vehicle in the European Union sets a target that 85% of the vehicle weight be either reused or recycled [1]. Natural fibres are mainly made of cellulose, hemicellulose, pectin, lignin and a small amount of extractives [2], and natural fibres such as flax, hemp, jute, sisal and ramie are commonly used as reinforcements in composites. Natural fibre composites seem to be one of the promising material systems used for auto parts manufacturing due to their low density, low price, ease of processing and biodegradability [2,3].

Usually, plant-based natural fibres have poorer mechanical properties than synthetic fibres such as glass fibres which are commonly used as reinforcements in composites. However, they may exhibit comparable or even better specific properties than glass fibres due to their low densities, which highlights that weight reduction is one of advantages for using natural fibre reinforced composites [4]. Thermoset and thermoplastic are two groups of polymer matrix composites. Compared to thermoset composites, the major advantages of thermoplastic composites are recyclability and the potential for rapid forming [5]. Polypropylene is an ideal matrix for natural fibres reinforcements due to its low price, low processing temperature and strong hydrophobic character [6].

Stamp forming is a frequently used forming technique to convert a sheet metal into a variety of thin automotive components and has been successfully to form lightweight material system such as fibre reinforced composites [7]. A number of studies have been carried out on analysing the forming behaviour of composites during stamp forming [7-9]. Sexton et al. [10] conducted stretch forming experiments on a fibre metal laminate system comprised of aluminium and a self-reinforced polypropylene composite. Comparison on FLD with 5005 H34 aluminium suggested that the laminate system can exhibit a superior formability compared to monolithic metal alloys.

Numerical simulations can help simulate the forming behaviour of material systems, and hence reduce trial and error part of product development. A large number of investigations have been conducted on simulating the forming behaviour of composites during rapid forming. Moss et al. [11] developed an FEA model simulating the behaviour of a fibre metal laminate based glass fibre reinforced polypropylene composite. Shell elements were used to model each layer of the fibre metal laminate structure and shear transfer stress between laminate layers predicted in the FEA simulation was justified properly with experimental results. Davey et al [12] developed a FEA model simulating the

forming behaviour of carbon fibre reinforced PEEK composite. In the model, Implicit FEA techniques were chosen over explicit technique, and a penalty friction condition was assigned to contacts between the composite and tools. The simulated strain evolution at the unsupported edge along 45° to off-fibre direction resembles the experimental data, indicating an accurately predicted material flow which is mainly influenced by the friction condition defined between the composite and tools.

2. Material preparation and experimental setup

This study investigated two composites with the same material constituents (flax and polypropylene), same thickness (1mm), similar weight fraction (approximately 50% in weight), but different weave structure (2 x 2 twill continuous woven composites and nonwoven short flax fibres reinforced structure). Continuous Natural Fibre Composite (NFC) fabric was manufactured by Composite Evolution, UK and then consolidated at Xiafei factory in China. Pre-consolidated Chopped Natural Fibre Composite (CNFC) was purchased from EcoTechnilin, UK. Composites were cut, painted and then tested from as-received material with no additional treatments.

By varying the aspect ratio of sample geometry, composite specimen is able to exhibit different major forming mode at pole. In order to investigate the material behaviour at different forming modes, hour glass geometries with varying middle section widths were used in this study. All specimens were cut through a mechanical scissors and dimensions were summarised in Table 1. Because of weave structure, continuous NFC specimens were cut such that fibres were oriented at 0/90° and 45/45° to the sample axis, respectively as shown in figure 1.

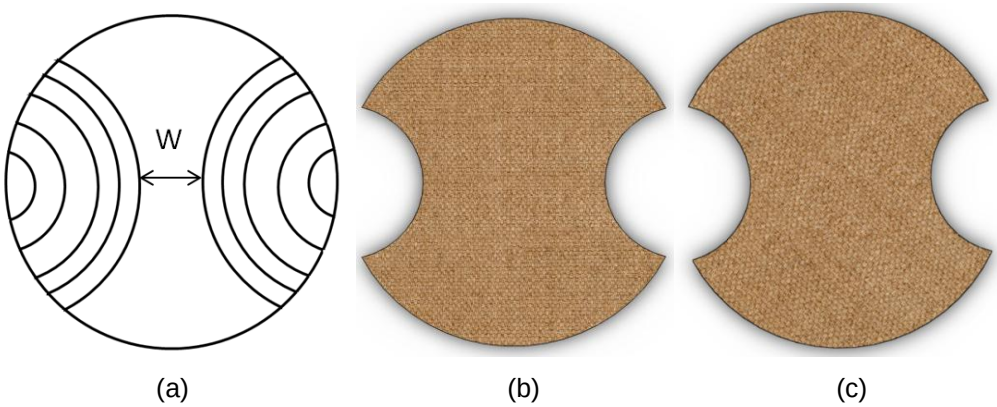

Figure 1: Illustration of specimen geometries (a) used in this study and different fibre orientation of NFC specimens, b. 0/90° specimen. c, 45/45° specimen.

Table 1: Dimensions of the specimens used in this study

Specimen	Width (mm)
W40mm	40
W55mm	55
W70mm	70
W100mm	100
W120mm	120
W200mm	200

The open die design of the stamping machine facilitated the application of the ARAMIS™ system to monitor the surface motion and to compute corresponding displacement and strain deformation. In

order to obtain the ideal condition for the ARAMIS™ system measurements, specimens were painted in a stochastic pattern of black dots on a white background before testing. Figure 2 shows the blank-holder and the die. Six M12 bolts were applied to fix the specimen in the fixture prior to forming and a 15kN.m tightening torque was chosen for all trials. No premature failure or composite movement at the lock-ring was detected at this tightening torque for all geometries used in this study, suggesting a reasonable amount of force applied to restrict the specimen during forming. Three layers of TEFLON were stacked together and placed on top of the specimen to lower the coefficient between the punch and the composite. This hinders the shift of the maximum strain deformation from the centre of the composite specimen to unsupported regions, resulting in a possible initiation of major cracks at the pole. This helps one establish the forming limit of this class of material system in a specific forming mode. A full field Forming Limit Curve (FLC) can be also obtained by establishing forming limits at different forming modes together, including biaxial stretch, plane strain, uniaxial tension, pure shear and wrinkling. In the experiment, the punch moved down at a constant rate of 20mm/s till the punch load drops to 80% of the maximum value due to composite failure.

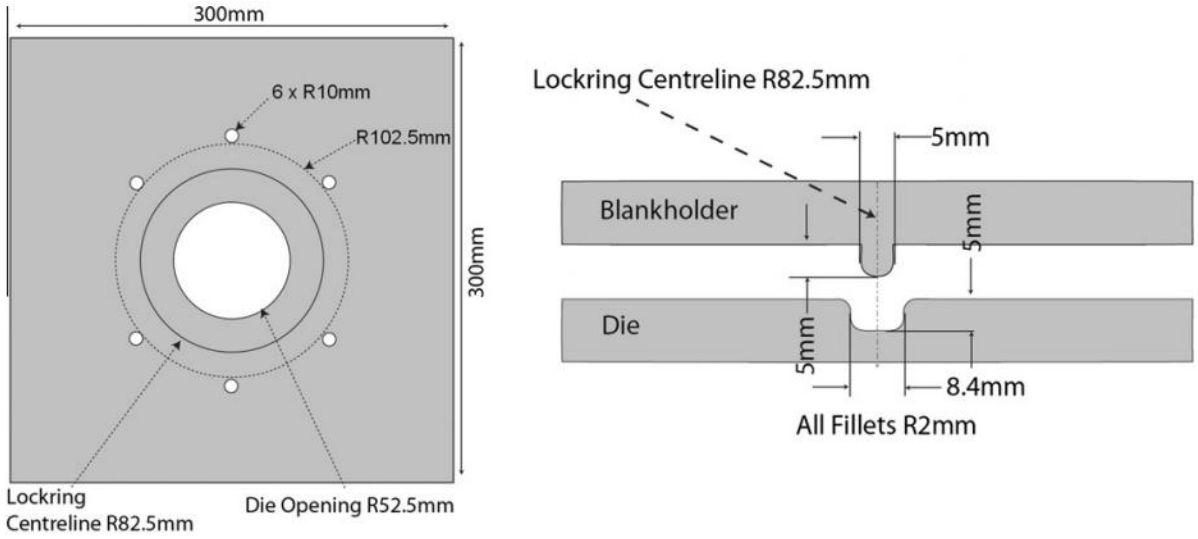

(a) (b)

Figure 2 The blank-holder (a) and the die (b), [11]

3. Finite Element Modelling

3.1 Material properties

The CNFC has a random distribution of chopped flax fibres and predominantly behaves quasi-isotropic. Through tensile tests on CNFC specimens with a dimension of 15mm by 150mm, the non-linear stress versus strain behaviour and the Poisson's ratio were obtained. These mechanical properties were translated to a non-linear stress strain relation and then assigned to the FEA model developed in this study. An orthotropic non-linear material behaviour was assigned to NFC specimens due to the weave structure of the composite. There are nine independent coefficients for an orthotropic material as shown in equation 1.

$$\begin{bmatrix}\sigma_{11}\\ \sigma_{22}\\ \sigma_{33}\\ \sigma_{23}\\ \sigma_{13}\\ \sigma_{12}\end{bmatrix} = \begin{bmatrix} C_{11} & C_{12} & C_{13} & 0 & 0 & 0 \\ C_{12} & C_{22} & C_{23} & 0 & 0 & 0 \\ C_{13} & C_{23} & C_{33} & 0 & 0 & 0 \\ 0 & 0 & 0 & C_{44} & 0 & 0 \\ 0 & 0 & 0 & 0 & C_{55} & 0 \\ 0 & 0 & 0 & 0 & 0 & C_{66} \end{bmatrix} \begin{bmatrix}\varepsilon_{11}\\ \varepsilon_{22}\\ \varepsilon_{33}\\ \varepsilon_{23}\\ \varepsilon_{13}\\ \varepsilon_{12}\end{bmatrix} \quad [1]$$

Similar to the CNFC, the material stiffness and the Poisson's ratio of the NFC were obtained through uniaxial tension tests along fibre orientations. The terms C_{11}, C_{22} and C_{12} were computed through micromechanics of a lamina as shown in equations 2-3. The in-plane shear stiffness, C_{66}, was

determined through the method introduced in [13]. C_{44} and C_{55} were computed through the correction factors suggested by ABAQUS as shown in equation 4 [14]. C_{13}, C_{23}, C_{33} were all zero as the FEA model used a thin shell formulation.

$$C_{11} = C_{22} = \frac{E}{1-v^2} \quad [2]$$

$$C_{12} = \frac{E*v}{1-v^2} \quad [3]$$

$$C_{44} = C_{55} = \frac{5}{6}C_{66} \quad [4]$$

3.2 Model parameters

Parts modelled in the simulation included a punch, a die, a blank-holder and a blank. Tools (the punch, the die and the blank-holder) were modelled as analytical rigid as they were much stiffer compared to composite and it is more likely that tools will penetrate the composite during forming rather than other way around. For the similar reason, tool surfaces and composite surfaces were modelled as master surface and slave surface, respectively, in contact conditions. Contact conditions have significant effects on material flow during forming, and a penalty contact was assigned to contacts between tools and the composite. A lower coefficient of friction was assigned to the contact between the punch and the composite due to the existence of three TEFLON layers. In the FEA model, the die stays stationary and the blank-holder was only allowed to move vertically to facilitate the action of Blank Holder Force (BHF). The punch was set to move down at a constant speed of 20mm/s to match with the actual experiment. The composite was meshed with shell elements with an approximate global element size of 4mm.

4. Results and discussions

4.1 Strain evolution at pole

The application of ARAMIS™ system allows the measurements of displacement and strain deformation at every point of material surface during forming. The pole of the specimen was in contact with the punch during forming. It experienced the maximum strain deformation, and it was likely that major cracks initiate in this region, especially when TEFLON layers were used. Strain evolutions at the pole were analysed to study the formability and forming limits exhibited in NFC and CNFC composites at different forming modes. Figures 2-3 show strain evolutions at the pole of specimens with varying middle section widths.

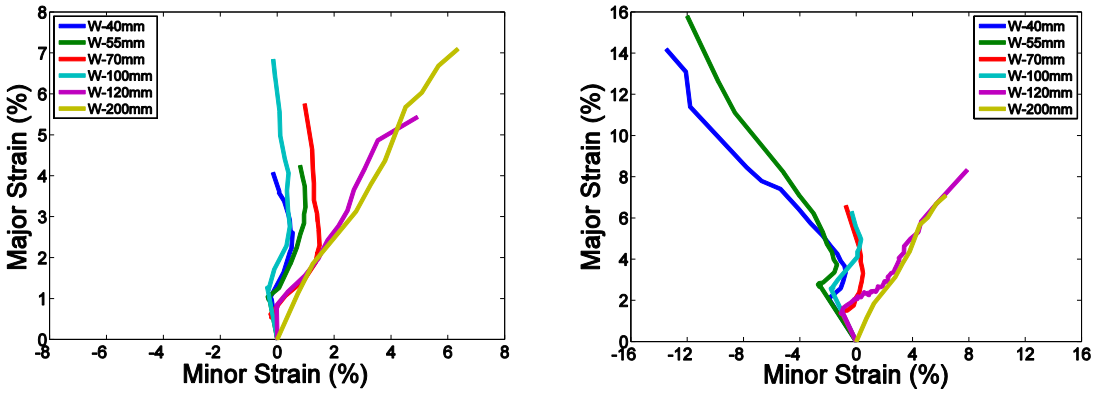

Figure 2: Strain evolutions at the pole of NFC specimens along (a) fibre orientations, (b) off-fibre orientations

Different slopes in the plot of major strain versus minor strain can represent varying forming modes, and observations on strain evolutions at the pole of NFC specimens suggest that stretch orientations can significantly change forming modes exhibited in NFC specimens. When NFC specimens are stretched along fibre directions (0/90° samples), forming modes exhibited in specimens include

uniaxial tension (α=-0.5), plane strain (α=0) and biaxial stretch (α=1). 45/45° NFC composites are able to exhibit an additional forming mode, pure shear (α=-1), at small widths (40mm and 55mm). It is also noticed that 45/45° specimens experience a significantly larger maximum strain deformation compared to 0/90° equivalent composites. In stretch forming experiments, not much material at the flange region draw into the die cavity as the edge of the composite is fixed completely to the lock-ring, suggesting that strain deformation exhibited in the specimen is closely related to forming depths. Fibre fracture is the dominant failure mechanism for this class of material system at room temperature [8]. Compared to 45/45 samples, flax fibres in 0/90 specimens are stretched a larger extend at similar forming depths, resulting in an early initiation of major cracks and hence a smaller maximum strain deformation. It is observed that sample geometry has a dominating effect over stretch directions for specimens with large widths as composites are forced to form in similar major forming modes at large restrictions in the lateral direction.

Strain evolution of the pole can be identified as three separate stages including pre-stretch, biaxial stretch and major forming path (composite exhibits its major forming modes at this stage). Specimens are fixed to the blank-holder through tightening six M12 bolts with a torque of 15kN.m on the lock-ring mounted beneath. In the pre-stretch state, sample is pulled on both edges, causing the composite to elongate in only the vertical direction. This results in a fairly uniform major forming mode of uniaxial tension in 0°/90° samples to pure shear in 45°/45° samples. For W200mm sample, the composite is pre-stretched evenly in all directions, exhibiting a major forming mode of biaxial stretch. The same tightening torque is applied to all trials conducted in this study and a larger strain deformation in the pre-stretch state can be expected on narrower samples where the same fixture force was applied to smaller regions. It is also observed that 45°/45° specimens exhibit a higher maximum strain deformation in the pre-stretch state compared to equivalent 0°/90° specimens. This can be attributed to a significantly higher stiffness along fibre orientations compared to 45˚ to them. When composites establish an initial contact with the punch in the biaxial stretch state, only the central region deforms and specimens exhibit a major forming mode of biaxial stretch. In this state, only a small region at the pole deforms and the material surface around the pole can be considered as fixed, resulting in a major forming mode of biaxial stretch during this period. This state ends when edges of the middle-section cannot facilitate stretch in the lateral direction, indicating a longer biaxial stretch state in larger samples. When the composite forms to a larger depth, it starts to exhibit its major forming path which is closely related to the aspect ratio of the composite. Strain ratios in the major forming path state are used to calculate specimens' deformation modes in this study. For 45°/45° specimens, the major strain path varies from pure shear (40mm and 55mm) to plane strain (70mm and 100mm) and further to biaxial stretch (120mm and 200mm). Again, the effect of stretch orientation is dominating over that of aspect ratio of sample geometry for those samples with small widths.

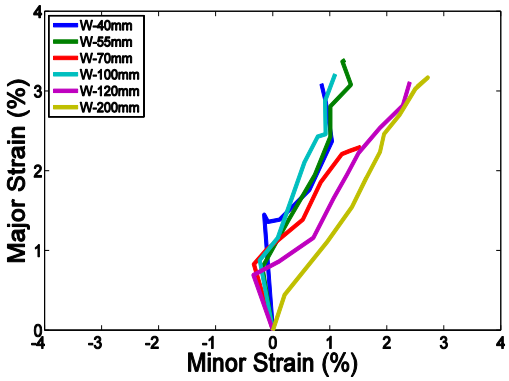

Figure 3: Strain evolutions at the pole of CNFC specimens

Similar to NFC, CNFC specimens experience a larger strain deformation in the pre-stretch state with decreasing in middle section widths. It is also observed from figure 3 that, except the narrowest sample (40mm), CNFC samples exhibit a major forming path close to biaxial stretch. CNFC composites can withstand a small amount of strain deformation before failure in rapid forming. As can be seen from strain evolutions, CNFC specimens exhibit a lower maximum major strain compared to NFC equivalent samples. It is likely that the CNFC experiences initiation of cracks in the initial contact state before exhibiting its major forming path. Therefore, it would be difficult to determine the effect of

weave structure on strain evolutions from specimens with large widths. CNFC composites are not able to exhibit a major forming mode of pure shear as even the narrowest sample experiences a major forming path of uniaxial tension. This is probably due to the quasi-isotropic nature of CNFC composites, and a similar observation found by Sexton et. al [11] that 5005 H34 aluminium can only exhibit forming modes varying from biaxial stretch to uniaxial tension in stretch forming.

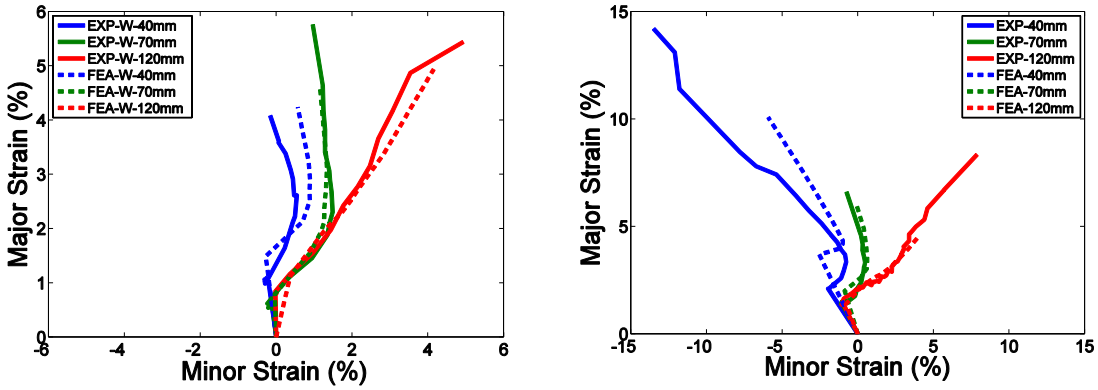

Figure 4: Strain evolution at the pole of NFC specimens from experimental results and FEA simulations along a. Fibre direction, b. Off-fibre direction

To validate FEA simulations developed in this study, three geometries with different widths (40mm, 70mm and 120mm) were selected to cover all forming modes exhibited in composites. Figures 4-5 show comparisons of strain evolutions at the pole between experimental results and FEA simulations, and strain evolutions of specimens with different widths can be simulated accurately by FEA simulations. It is also important to know that strain evolutions from FEA simulations can correctly predict the progress of major forming path, for both NFC and CNFC. Therefore, material properties assigned to deformable blank and friction conditions defined between contacts appear to be accurate. In FEA simulations, the composite was modelled as a homogeneous material which exhibits same mechanical properties at every single mesh node of the surface. However, the composite does not behave ideally homogeneously due to variation in mechanical properties caused by the uneven thickness of composites and the existence of voids. This can explain the slight discrepancy between experimental findings and FEA simulations.

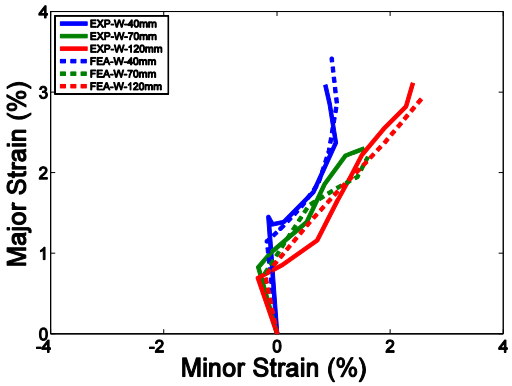

Figure 5: Strain evolutions at the pole of CNFC specimens

4.2 Punch load versus displacement curves

The punch load versus displacement curve is an indicative of the amount of energy absorbed by the specimen, and more importantly, can provide insights to material behaviour during forming. Similar to the previous section, punch load curves of three geometries with widths of 40mm, 70mm and 120mm were chosen to compare with FEA simulations. These geometries were chosen because they can cover entire forming modes exhibited in all sample geometries.

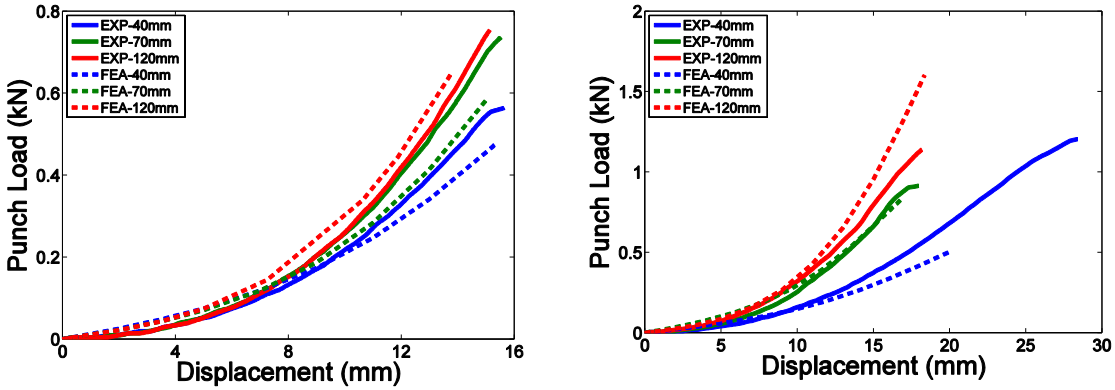

Figure 6: Punch load versus displacement of NFC specimens from experimental results and FEA simulations along a. Fibre direction, b. Off-fibre direction

Figure 6 illustrates comparisons of punch load curves obtained from experimental results and FEA simulations. Compared to 0°/90˚ specimens, 45°/45˚ samples can form to a larger depth due to the significantly larger elongation-to-failure along shear directions than fibre directions. However, it is noted that 0°/90˚ and 45°/45˚ specimens with a width of 120mm share a similar evolution of the punch load prior to a forming depth of 15mm, experiencing punch load forces of 0.74kN and 0.79kN, respectively. For 0°/90˚ NFC samples, there is an increase in amount of energy required to form composites when sample width increases. This can be attributed to the increase in the forming area and the amount of material squeezed at the flange region during forming. A similar trend can be identified from 45˚/45˚ NFC composites, with a significantly larger increase between W40mm and W55mm specimens. This agrees with the findings obtained from the previous section that the stretch orientation has a dominating effect over sample geometry at small widths. Shear stiffness is much lower than fibre stiffness due to the weave structure, and hence 45°/45° samples require less amount of energy compared to 0°/90° specimens. CNFC samples exhibit a similar trend in punch load curves compared to 0˚/90˚ NFC composites. There is a distinct increase in punch load when the sample width increases from 40mm to 70mm, and then to 120mm. FEA simulations developed can accurately predict the punch load curves for samples with different widths, and also correctly simulate the effect of stretch orientation for NFC composites.

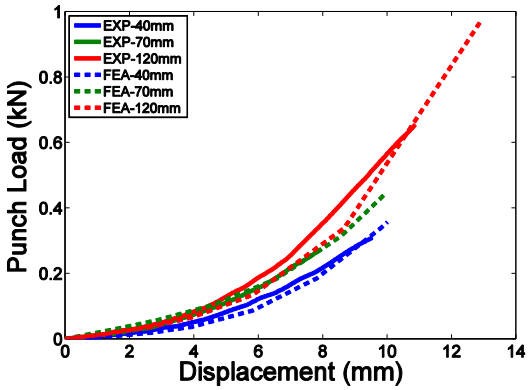

Figure 7: Punch load versus displacement of CNFC specimens from experimental results and FEA simulations

4. Conclusion

This study analyses the forming behaviour of flax fibre reinforced polypropylene composites, and investigates the effect of weave structure on this class of material system in stamp forming. The finite element models developed in this study correlate well with experimental observations in strain evolutions at the pole and punch load curves. It is found that sample geometry has a dominating effect over stretch orientation for samples with small widths. It is also observed that the woven natural fibre

composite is able to exhibit a major forming path of pure shear which cannot be observed from nonwoven composites. Good correlation between experimental observations and FEA simulations is obtained in this study.

References

1. A.R. Dickson, D. Even, J.M. Warnes, A. Fernyhough, 2014, “The effect of reprocessing on the mechanical properties of polypropylene reinforced with wood pulp, flax or glass fibre,” *Composites: Part A,* vol. 61, pp. 258-267
2. Y. Xie, C.A.S. Hil, Z. Xiao, H. Militz, C. Mai, 2010, “Silane coupling agents used for natural fiber/polymer composites: A review,” *Composites: Part A,* vol. 41 no. 7, pp. 806–819.
3. A.C.N Singletona, C.A. Baillieb, P.W.R Beaumonta, and T. Peijs, 2003, “On the mechanical properties, deformation and fracture of a natural fibre/recycled polymer composite,” *Composites: Part B* vol. 34 no.6, pp. 519–526.
4. F. Duc, P.E. Bourban, C.J.G. Plummer, J.A.E. Manson, 2014, “Damping of thermoset and thermoplastic flax fibre composites,” *Composites: Part A,* vol. 64, pp. 115-123.
5. Hou M. 1997, “Stamp forming of continuous glass fibre reinforced polypropylene”, Composite Part A, vol. 33, pp. 695-702.
6. Garkhail SK, Heijenrath RWH, Peijs T. 2000, “Mechanical properties of Natural-Fibre-Mat-Reinforced Thermoplastic based on Flax Fibres and Polypropylene”, Applied Compos Material, vol. 7, pp. 351-372.
7. S. Kalyanasundaram, S. DharMalingam, S. Venkatesan, A. Sexton. 2013, “Effect of process parameters during forming of self-reinforced – PP based Fibre Metal Laminate,” *Composite Structures*, vol. 97 pp. 332-337.
8. W. Wang, A. Lowe, S. Kalyanasundaram. 2013, “A study on continuous flax fibre reinforced polypropylene composite in stamp forming process.” *Advanced Composites Letters*, vol. 22, pp. 86-89.
9. J. Gresham, WJ. Cantwell, M. Cardew-Hall, P. Compston, S. Kalyanasundaram. 2006, “Drawing behaviour of metal–composite sandwich structures,” *Composite Structures*, vol. 75, pp. 305–312.
10. A. Sexton, W. Cantwell, MJ. S. Kalyanasundaram. 2012, “Stretch forming studies on a fibre metal laminate based on a self-reinforcing polypropylene composite,” Composite Structures,” vol. 94, pp. 431–437.
11. L. Mosse, P. Compston, W.J. Cantwell, M. Cardew-Hall, S. Kalyanasundaram. “The development of a finite element model for simulating the stamp forming of fibre-metal laminates,” *Composite Structures*, vol. 75, pp. 298-304.
12. S. Davey, R. Das, WJ. Cantwell, S. Kalyanasundaram. “Forming studies of carbon fibre composite sheets in dome forming processes,” *Composite Structures*, vol. 97, pp. 310–316.
13. D. Gay, S.V. Hoa, S.W. Tsai, 2003, “Composites Materials - Design and Applications” CRC Press LLC, Paris, PP:442, Cha:18.
14. Abaqus analysis user’s manual, Version 6.9. Hibbitt: Karlsson & Sorensen; 2009.

.